Physical Origins and Analysis of Negative-Bias Stress Instability Mechanism in Polymer-Based Thin-Film Transistors

Jaewook Lee, Jaeman Jang, Hyeongjung Kim, Jiyoul Lee, Bang-Lin Lee, Sung-Jin Choi,
Dong Myong Kim, *Member, IEEE*, Dae Hwan Kim, *Senior Member, IEEE*,
and Kyung Rok Kim, *Member, IEEE*

Abstract—The physical origins of the negative-bias stress (NBS) instability in polymer-based thin-film transistors have been characterized. Through the quantitative analysis by TCAD simulation for the NBS time-dependent experimental results, the threshold voltage (V_T)-shift by sub-bandgap density-of-states redistribution forms 70% and 78% for the measured total V_T-shift while V_T-shift by gate oxide charge trapping only takes 30% and 22% at NBS time of 3000 and 7000 s, respectively. In addition, the increase of source/drain Schottky contact resistance (R_{SD}) is the main reason for NBS-induced ON-current (I_{ON}) degradation.

Index Terms—Negative-bias stress, instability, polymer, thin-film transistor, density-of-states, redistribution, threshold voltage, ON-current degradation, Schottky contact resistance.

I. INTRODUCTION

ORGANIC electronic technology has been extensively developed to be used in the various applications such as flexible active-matrix displays, radio-frequency identification, non-volatile memory, microelectronic circuits, and biochemical sensors. In particular, the development of the high-performance polymer-based thin-film transistors (TFTs) based on solution process provides a great opportunity to implement flexible electronic circuits using the inkjet printing technology. Recent research works have reported polymer TFTs (PTFTs) with high mobility [1]–[3], which can extend the applications of the high-performance printed electronics.

Besides high mobility in PTFTs, bias stress instability is the important issue that should be improved for the mass produc-

tion of the PTFT-based printed electronic circuits. Therefore, it is essential to characterize quantitatively the main origins of the instability under various bias stress conditions for the reliable performance of PTFTs in the engineering aspects. Quantitative analysis for the instability, however, has been rarely reported while there have been a lot of works for high mobility PTFTs. Although previous studies for bias stress instability analyzed the positive charge (hole) trapping into gate insulator or its interface as the main origin of stress-induced instability [4], [5], the quantitative investigation and analysis for its correlated factors is the urgent research that should be performed in advance since the physical origins of the bias stress-induced instability strongly interact in the actual polymer semiconductor devices.

In this letter, we characterized the dominant physical origins of the negative bias stress (NBS) instability mechanism in the thiophene-based high-performance PTFTs by reproducing the NBS time (t_{NBS})-dependent experimental characteristics using numerical TCAD device simulation. For quantitative analysis, sub-bandgap density-of-states (DOS) in the polymer channel of the fabricated PTFTs are extracted from the monochromatic photonic capacitance-voltage (MPCV) technique [6] according to the various t_{NBS}. Then, in addition to the charge trapping into the gate oxide and interface, the effects of DOS redistribution and the source/drain contact resistance (R_{SD}) on the NBS instability will be discussed as the main origins quantitatively.

II. DEVICE FABRICATION AND NBS CHARACTERISTICS

For the p-channel layer of PTFT, polymer semiconductor (poly (tetryldodecyloctathiophene-*alt*-didodecylbithiazole-co-tetryldodecylhexathiophene-*alt*-didodecylbithiazole), P(8T2Z-co-6T2Z)-12) was dissolved in tetra-hydronaphthalene (THN) at a concentration of 0.2 wt%, and then inkjet-printed via Dimatix printer onto the coplanar structured PTFTs fabricated on a glass substrate as shown Fig. 1. The fabricated PTFTs have the channel width (W) of 120 μm, length (L) of 8 μm, gate-to-S/D overlap length (L_{OV}) of 10 μm, gate oxide thickness (T_{OX}) of 300 nm, and polymer film thickness $(T_{polymer})$ of 30 nm.

Considering this coplanar structure, large negative bias from bottom-gate can increase the effective Schottky barrier height (ϕ_{bo}) for hole injection by $\Delta\phi_{bo}$ due to the hole trapping in contact interface or subgap DOS in the channel
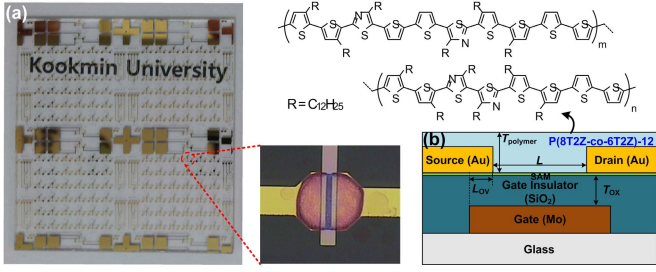
Fig. 1. (a) Top view of the fabricated PTFT on glass substrate using inkjet printing technology. (b) Cross-sectional schematic of the fabricated coplanar (bottom-gate/bottom source/drain contacts) PTFT having thiophene-based polymer channel material (P(8T2Z-co-6T2Z)-12) and its chemical structure.
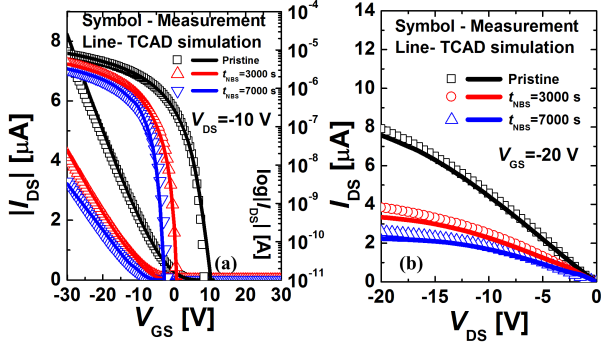

Fig. 2. Measured and simulated I-V results of the fabricated PTFT having $W/L = 120/8$ μm by NBS conditions: (a) Transfer I_{DS}-V_{GS} characteristics at $V_{DS} = -10$ V. (b) Output I_{DS}-V_{DS} characteristics at $V_{GS} = -20$ V. On-current degradation and V_T shift in a negative direction from measurement (symbols) have been reproduced by TCAD simulation (lines) according to the increase of $t_{NBS} = 0$ (pristine), 3000 s, and 7000 s at $V_{GS} = -20$ V.

during tunneling from source to channel since NBS conditions have been applied with the current flowing on-state ($V_{GS} = -20$ V, $V_{DS} = -10$ V). The measured transfer and output I-V curves of the fabricated PTFT, as shown in Fig. 2(a) and (b) (symbols), obviously indicate the on-current degradations according to the increase of t_{NBS}. The PTFT model-incorporated TCAD simulation well reproduced these on-current degradations through Schottky contact surface current model as

$$J_{SP} = qv_{SURFP}\left(P_S - P_{eq}\right)\exp\left(-\frac{q\phi_{bo}}{kT}\right),$$

$$v_{SURFP} = \frac{ARICHP \cdot T_L^2}{qN_V} \qquad (1)$$

where hole surface recombination velocity $v_{SURFP}=3.3\times10^5$ cm/s with hole Richardson constant $ARICHP = 30$ Acm^{-2}K^{-2} (default) assuming $N_V = 5\times 10^{19}$ cm^{-3} and $T_L = 300$ K, P_S is surface hole concentration, and P_{eq} is equilibrium hole concentration [7], [8]. For the transport through the polymer channel, the electric field-dependent Poole-Frankel (PF) mobility model including DOS-dependent variable range hopping (VRH) mobility and Langevin recombination model have been used in TCAD simulation [9]. From the well-calibrated TCAD simulation (lines in Fig. 2), ϕ_{bo} can be determined as 0.36, 0.46, and 0.5 eV for t_{NBS} of 0 (pristine), 3000 s, and 7000 s, respectively.
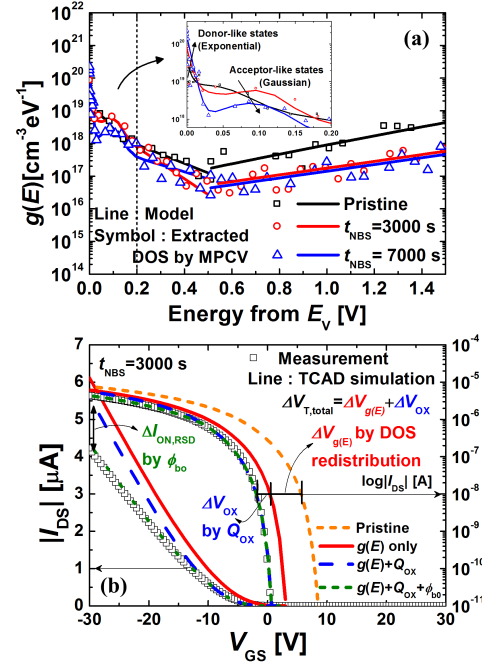

Fig. 3. (a) The extracted DOS distributions (symbols) from MPCV method and calculated ones (lines) from DOS model as a function of an energy from E_v for pristine, $t_{NBS} = 3000$ s, and 7000 s. Inset shows the detailed $g_{DA}(E)$ and $g_{TD}(E)$ profiles near E_v upto 0.2 eV. (b) Linear and log scale I_{DS}-V_{GS} plots at $V_{DS} = -10$ V for $t_{NBS} = 3000$ s. TCAD simulation results (lines) characterize the origins of NBS-induced ΔV_T and ΔI_{ON} by using physical models during approaching the measurement ones (symbols).

Moreover, from $\log|I_{DS}|$-V_{GS} plots in Fig. 2(a), it should be noted that the threshold voltage (V_T) of p-channel PTFT has been shifted to a negative V_{GS} direction as t_{NBS} increases. The main physical origins of these significant V_T shifts under the time-dependent NBS conditions will be investigated by considering the subgap DOS distribution in the polymer channel as well as charge trapping in the gate insulator and its interface.

III. RESULTS AND DISCUSSION

Fig. 3(a) shows the distributions of the subgap DOS ($g(E)$) as a function of an energy from the valence band maximum (E_v) of the polymer semiconductor. The experimentally extracted $g(E)$ distributions from the reproducible MPCV technique based on the equivalent circuit model with C-V measurement [6] indicate that the acceptor-like deep states $g_{DA}(E)$ of Gaussian profiles with the peak energy (E_{DA}) are suppressed moving toward mid-gap from $E_{DA} = 0.05$ eV to 0.1 eV and the exponential donor-like tail states $g_{TD}(E)$ near the band edge (E_v) increase as t_{NBS} is applied and increased [inset of Fig. 3(a)]. The physical origin of $g_{TD}(E)$ increase in the polythiophene material can be attributed to the ammonia donors (NH$_4^+$) enhanced by the hole accumulation at the surface under the on-state NBS conditions [10]. In terms of $g_{DA}(E)$, which has the consistent results of $E_{DA} \sim 0.1$ eV [10], it should be noted that this $g_{DA}(E)$ redistribution by NBS has been experimentally observed for the first time. Therefore, more rigorous physical origin of NBS-induced $g_{DA}(E)$ decrease would be validated as further research besides ozone (O$_3$) as the well-known origin of the accepter states [11]. In the present work, all these experimental

TABLE I
NBS TIME EVOLUTION OF SUBGAP DOS PARAMETERS

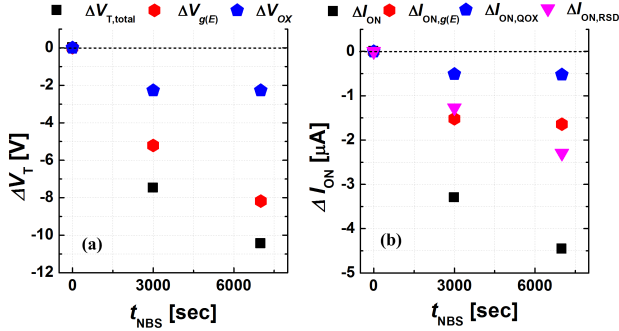| Stress Time	Pristine	t_{NBS}=3000 s	t_{NBS}=7000 s
N_{TD} [cm^{-3}eV^{-1}]	2.5×10^{19}	7×10^{19}	1.5×10^{20}
kT_{TD} [eV]	0.0021	0.005	0.005
N_{DA} [cm^{-3}eV^{-1}]	5×10^{18}	3.5×10^{18}	2×10^{18}
kT_{DA} [eV]	0.055	0.038	0.05
E_{DA} [eV]	0.03	0.1	0.09

Fig. 4. The characterization results for the physical origins of the NBS-induced (a) $\Delta V_{T,total}$ as $\Delta V_{T,total} = \Delta V_{g(E)} + \Delta V_{OX}$ and (b) ΔI_{ON} as $\Delta I_{ON} = \Delta I_{ON,g(E)} + \Delta I_{ON,QOX} + \Delta I_{ON,RSD}$ according to the increase of t_{NBS}.

DOS redistributions of $g_{DA}(E)$ and $g_{TD}(E)$ are well fitted with the acceptable error margins by DOS model as [6]

$$g_{DA}(E) = N_{DA} \exp\left(-\frac{E_{DA} - E}{kT_{DA}}\right)^2,$$

$$g_{TD}(E) = N_{TD} \exp\left(\frac{E_V - E}{kT_{TD}}\right) \qquad (2)$$

where N_{DA} (N_{TD}) and kT_{DA} (kT_{TD}) are the effective density of states and the characteristic energy for the acceptor-like deep (donor-like tail) states, respectively. Since DOS redistributions close to E_v cause more V_T-shift than those far from E_v in a p-channel PTFT [10], V_T-shift by $g(E)$ redistribution $\Delta V_{g(E)}$ should be considered as the physical origin of the NBS-induced total V_T-shift ($\Delta V_{T,total}$) by focusing on $g_{DA}(E)$ and $g_{TD}(E)$ with the parameters for thiophene-based polymers as in Table I.

As shown in Fig. 3(b), by incorporating only the redistributed $g(E)$ model for $t_{NBS} = 3000$ s into TCAD simulation, we obtained $\Delta V_{g(E)} = -5.21$ V (about 70 % of the measured $\Delta V_{T,total} = -7.48$ V), which is larger than V_T-shift by the charge trapping in gate oxide (ΔV_{OX}) even assuming $\Delta V_{T,total} - \Delta V_{g(E)} = \Delta V_{OX}$. Therefore, it should be noted that subgap DOS redistribution is the dominant physical origin for the NBS-induced $\Delta V_{T,total}$ in PTFTs rather than the trapped charge in the gate oxide (Q_{OX}). On the other hand, as noted in the linear scale I_{DS}-V_{GS} plots of Fig. 3(b), the main reason of the on-current degradation (ΔI_{ON}) is the increase of R_{SD} (resulting from $\Delta \phi_{bo}$) as discussed in Section II because $\Delta I_{ON,RSD}$ by the change of R_{SD} should be substantially included for reproducing the measured $I_{ON}(t_{NBS})$ in the form of $\Delta I_{ON} = \Delta I_{ON,g(E)} + \Delta I_{ON,QOX} + \Delta I_{ON,RSD}$, taking into accounts the effect of ΔV_T on ΔI_{ON}, i.e., $\Delta I_{ON,g(E)}$ by $\Delta V_{g(E)}$ and/or $\Delta I_{ON,QOX}$ by ΔV_{OX}. In terms of $\Delta I_{ON,g(E)}$,

mobility degradation by $g_{TD}(E)$ increase near the band edge has been considered by DOS-dependent VRH mobility model in TCAD simulation as well.

All of the physical origins of the NBS-induced $\Delta V_{T,total}$ and ΔI_{ON} for various t_{NBS} have been quantitatively illustrated in Fig. 4. For the characterizations of $\Delta V_{T,total}$ [Fig. 4(a)], $\Delta V_{g(E)}$ by DOS redistribution forms 69.6 % at $t_{NBS} = 3000$ s, and 78.3% at $t_{NBS} = 7000$ s while ΔV_{OX} by Q_{OX} only takes the rest of 30.4 % and 21.7%, respectively. As shown in Fig. 4(b), $\Delta I_{ON,RSD}$ by the increase of R_{SD} becomes dominant for ΔI_{ON} as t_{NBS} increases compared with $\Delta I_{ON,g(E)}$ by both negative V_T-shift ($\Delta V_{g(E)}$) and mobility degradation from NBS-induced DOS redistribution.

IV. CONCLUSION

Differently from well-known mechanism in organic TFTs, *i.e.*, charge trapping, we found the dominant physical origins of the NBS instability in the thiophene-based PTFTs as DOS redistributions near E_v for V_T-shift as well as the R_{SD} increase for I_{ON} degradation. The quantitative analysis has been performed through the comparison between the experimental results and TCAD simulations, which carefully incorporate the DOS distribution and Schottky contact model. These distinguished results for the main physical origins of NBS-induced instability indicate that even though gate insulator and its interface with the channel polymer semiconductor have been improved by solution process in the high-performance PTFTs, the additional optimization of subgap DOS and contact resistance are essential for the reliability of high-performance PTFTs.

REFERENCES

[1] H. Yan, Z. Chen, Y. Zheng, *et al.*, "A high-mobility electron-transporting polymer for printed transistors," *Nature*, vol. 457, no. 6, pp. 679–686, Feb. 2009.
[2] H. Sirringhaus, "Device physics of solution-processed organic field-effect transistors," *Adv. Mater.*, vol. 17, no. 20, pp. 2411–2425, Oct. 2005.
[3] J. Lee, J. W. Chung, J. Jang, *et al.*, "Influence of alkyl side chain on the crystallinity and trap density of states in thiophene and thiazole semiconducting copolymer based inkjet-printed field-effect transistors," *Chem. Mater.*, vol. 25, no. 9, pp. 1927–1934, Apr. 2013.
[4] J. Lee, D. H. Kim, B.-L. Lee, *et al.*, "Characterization of bias stress induced electrical instability in liquid-crystalline semiconducting polymer thin-film transistors," *J. Appl. Phys.*, vol. 110, no. 8, pp. 084511-1–084511-5, Oct. 2011.
[5] Y. R. Liu, R. Liao, P. T. Lai, *et al.*, "Bias-stress-induced instability of polymer thin-film transistor based on poly(3-Hexylthiophene)," *IEEE Trans. Device Mater. Rel.*, vol. 12, no. 1, pp. 58–62, Mar. 2012.
[6] H. Bae, H. Choi, S. Jun, *et al.*, "Single-scan monochromatic photonic capacitance-voltage technique for extraction of subgap DOS over the bandgap in amorphous semiconductor TFTs," *IEEE Electron Device Lett.*, vol. 34, no. 12, pp. 1524–1526, Dec. 2013.
[7] *ATLAS Device Simulation Software User's Manual*, SILVACO Int., Santa Clara, CA, USA, 2009.
[8] C. R. Crowell and S. M. Sze, "Current transport in metal-semiconductor barriers," *Solid-State Electron.*, vol. 9, no. 11, pp. 1035–1048, Nov. 1966.
[9] J. Kim, J. Jang, M. Bae, *et al.*, "Characterization of density-of-states in polymer-based organic thin film transistors and implementation into TCAD simulator," *J. Semicond. Technol. Sci.*, vol. 13, no. 1, pp. 43–47, Feb. 2013.
[10] R. A. Street, M. L. Chabinyc, and F. Endicott, "Chemical impurity effects on transport in polymer transistors," *Phys. Rev. B*, vol. 76, no. 11, pp. 045208-1–045208-9, Jul. 2007.
[11] M. L. Chabinyc, R. A. Street, and J. E. Northrup, "Effects of molecular oxygen and ozone on polythiophen-based thin-film transistors," *Appl. Phys. Lett.*, vol. 90, no. 12, pp. 123508-1–123508-3, Mar. 2007.